

# Effect of pH, Amount of Metal Precursor, and Reduction Time on the Optical Properties and Size of Zinc Oxide Nanoparticles Synthesized Using Aqueous Extract of Rhizomes of *Acorus calamus*

Melina Tamang<sup>1</sup>, Kamal Prasad Sapkota<sup>2</sup>, Sabita Shrestha<sup>2\*</sup>

<sup>1</sup>Department of Chemistry, Amrit Science College, Thamel, Kathmandu, Nepal

<sup>2</sup>Central Department of Chemistry, Tribhuvan University, Kirtipur, Kathmandu, Nepal

\*Corresponding E-mail: shresthasabita@hotmail.com

Submitted 12/09/2022, revised: 07/29/2023, accepted: 08/10/2023

## Abstract

Nanoparticles possess various unique characteristics compared to the corresponding bulk materials. Large band gap, non-toxic nature, and multi-applicability are the worthwhile characteristics of zinc oxide to be synthesized and studied. The size of nanoparticles can be controlled by varying the different experimental conditions. This paper reports the synthesis of zinc oxide nanoparticles by using an aqueous extract of rhizomes of *Acorus calamus*, where the bio-components present in aqueous extract acted as reducing agents. The size and band gap energy of zinc oxide nanoparticles were studied by varying different parameters such as pH, concentration of the metal precursor, and reduction time. The variations in the size of nanoparticles were studied by UV-visible spectroscopy. FTIR showed phenolic compounds, primary amines, and amides (proteins/enzymes) as the functional groups responsible for the reduction of metal precursors to form nanoparticles. The surface morphology of nanoparticles was studied by FE-SEM image. The FE-SEM image displayed the formation of various shapes and agglomeration of the nanoparticles. XRD pattern revealed that the average size of zinc nanoparticles is 10 nm. *In vitro* antibacterial activity of ZnO nanoparticles has been assayed against gram-positive and gram-negative bacteria. The growth inhibitory activity of nanoparticles against different bacterial pathogens has also been determined.

**Keywords:** *Acorus calamus*; Antibacterial agent; green synthesized nanoparticles

## Introduction

Nanotechnology, over the years, has drawn remarkable attention. It deals with the processes that occur at the molecular level and of nano-length scale size [1]. Nanoparticles show atom-like behavior

whose size ranges between 1-100 nm. The atom-like behavior is due to the higher surface area and wider band gap between valence and conduction bands when divided to near atomic size [2]. They show certain properties that make them different from that of bulk

materials such as large fractions of surface atoms, high surface energy, spatial confinement, and reduced imperfections. Oxide semiconductor nanostructures have been widely investigated in recent years as they show excellent electrical and optical properties, highly useful in the fabrication of nano-scaled optoelectronic and electronic devices with multi-functionality [3].

Nano-sized zinc oxide materials are one of the most versatile materials with forefront use in research studies [4]. Additionally, ZnO is an important n-type semiconductor with tremendous scientific and technological interest with a band gap of 3.37 eV and a large exciton binding energy of 60 MeV [5]. It has been reported as a highly preferred multi-tasking metal oxide having a vast list of attractive properties. Zinc oxide nanoparticles show non-toxicity, chemical stability towards high temperature and ultra-violet rays, and antibacterial and antifungal properties [6, 7]. They have a wide range of applications such as in pharmaceuticals, bio-molecular, and diagnostics, biosensors, photo-catalysts, photo-detectors, gas sensor devices, nano-generators, cosmetics, solar cells, water-purifier removing arsenic and sulfur and microbial inhibition [8-17]. Furthermore, zinc oxide nanoparticles can be accounted as one of the most prominent and promising agents for cancer treatment, exhibiting toxicity to human cancer cells after targeted delivery [18].

Synthesis of nanoparticles through plant extracts is a green chemistry approach interconnecting nanotechnology and plant biotechnology. The extract from different parts of the plant is used for bio-reduction of metal ions to nanoparticles. Bio-reduction is the process in which metal ions are reduced to metal atoms by plant-based biogenic reducing agents and several water-soluble plant metabolites. This synthesis exhibits superiority over the chemical method. The twelve principles of green

chemistry have now become a reference guide for researchers, scientists, and chemists globally to generate less toxic chemical products and byproducts [19]. Since green synthesis uses benign materials like leaf extract of plant, bacteria, fungi and enzymes, it offers various benefits such as eco-friendliness and compatibility for pharmaceuticals and other bio-medical applications [20-23].

The plant phytochemicals with antioxidant properties are accountable for the preparation of metal and metal oxide nanoparticles. Recently, biosynthesis of zinc oxide nanoparticles using extract of *Costus pictus*, lemongrass leaves, *Corymbia citriodora*, *Ruta graveolens*, *Aloe vera* and *Hibiscus sabdariffa*, *Garcinia mangostana*, *Streptomyces sp.*, *Ulva lactuca*, *Allivum sativum*, *Nigella Sativa L.* extract has been reported [24-33].

*Acorus calamus* is commonly called Bojho in the Nepali language. It belongs to the Acoraceae family. It is a perennial plant whose parts such as leaves, roots, and stems have been used to cure various diseases such as fever, asthma, bronchitis, and digestive disorders. It has been also used as a sedative [34]. The presence of various phytochemicals such as alkaloids, flavonoids, terpenoids, steroids, proteins, and carbohydrates is responsible for the reduction of zinc nitrate and the formation of zinc oxide nanoparticles [35].

## Materials and Methods

### Collections of sample

The fresh rhizomes of *Acorus calamus* were collected from Dang Valley of Nepal, which lies at 28° 7' 0 N Latitude, 82° 17' 60 E Longitude, and 628 meter altitude. Rhizomes were cut into small pieces, dried, and powdered by using a disk mill. Zinc nitrate hexahydrate [ $Zn(NO_3)_2 \cdot 6H_2O$ ] was purchased from Fischer Scientific (99.8 % purity). Bacterial cultures

of *E. coli*, *S. typhimurium*, *S. aureus*, and *K. pneumonia* were obtained from the National Institute of Science and Technology (NIST), Sohrakutte, Kathmandu.

### Preparation of aqueous extract

Powdered rhizome of the *Acorus calamus* (10 g) was taken in a conical flask and distilled water (100 mL) was added to it. It was then kept in a water bath at 60 °C for 30 minutes. Further, it was filtered using a muslin cloth, centrifuged, and again filtered using Whatmann filter paper. Thus, the filtrate was ready for further use.

### Green synthesis of nanoparticles

The aqueous extract of the *Acorus calamus* was used for the bio-reduction of zinc nitrate solution, which was used as a precursor for the synthesis of zinc oxide nanoparticles.

Zinc nitrate solution (100 mL, 5 mM) was taken and aqueous extract of *Acorus calamus* (30 mL) was added, followed by constant stirring at 60 °C using a magnetic stirrer. A pale yellow precipitate was obtained after constant stirring for 4 hours which was washed with distilled water followed by centrifugation at 4000 rpm for 10 minutes. Thus obtained precipitate was calcined at 400 °C for 2 hours.

### Characterization ZnO nanoparticles

The room temperature UV-visible absorption spectra of the samples were measured in a UV-visible spectrophotometer (Model LT2802). FTIR spectra of the extract and synthesized zinc oxide nanoparticles were recorded in Fourier Transform Infrared Spectrometer (FTIR, Tracer-100). X-ray diffraction (XRD, Rikagu Japan) using Cu K $\alpha$  ( $\lambda = 1.54\text{\AA}$ ) radiation and Bragg's angle ( $2\theta$ ) in the range of 5° to

90° was used for revealing the crystal structure of the zinc oxide nanoparticles. Field Emission Scanning Electron Microscopy (FE-SEM, Carl Zeiss Supra-40 VP, Germany) was used to investigate the structural morphology of zinc oxide nanoparticles.

### Evaluation of antibacterial activity

Antibacterial activity refers to the ability of the nanoparticles to kill or inhibit the growth of pathogenic microorganisms. The antibacterial screening of nanoparticles was carried out by the agar well diffusion method [36]. It was carried against four bacterial strains *Escherichia coli*, *Salmonella typhimurium* and *Klebsiella pneumonia* (Gram-negative bacteria) and *Staphylococcus aureus* (Gram-positive bacteria).

25 mg/mL concentration of the working solution was prepared by diluting 50 mg/mL stock solution of nanoparticles dispersed in DMSO. Active cultures of bacteria were cultured in nutrient broth, and incubated for 24 hours at 37 °C. Sterile Muller-Hilton Agar plates were prepared and wells were made in the incubated media plate with the help of sterile cork borer (4 mm) and labeled. 15  $\mu\text{L}$  of the working solution of nanoparticles was loaded in the respective well with the help of a micro-pipette. Neomycin was used as the positive control and tested for its activity at the same time. Plates were incubated for 6 hours at 37 °C. After proper incubation, the plates were observed for the Zone of Inhibition (ZOI) around the well. The ZOIs were measured with the help of a ruler and the mean was recorded for the estimation of potency of antibacterial substance.

## Results and Discussion

### UV-Vis Spectral analysis

UV- Visible spectroscopy is one of the important characterization techniques to study the synthesized nanoparticles. Fig. 1 shows the room temperature UV-visible spectrum of ZnO NPs synthesized using the green method from Rhizomes extract of *Acorus calamus*. The UV- VIS spectroscopy revealed the formation of ZnO nanoparticles by exhibiting the typical Surface Plasmon Resonance absorption peak centered at 365 nm and the similar results are reported in the previous research works [37, 38].

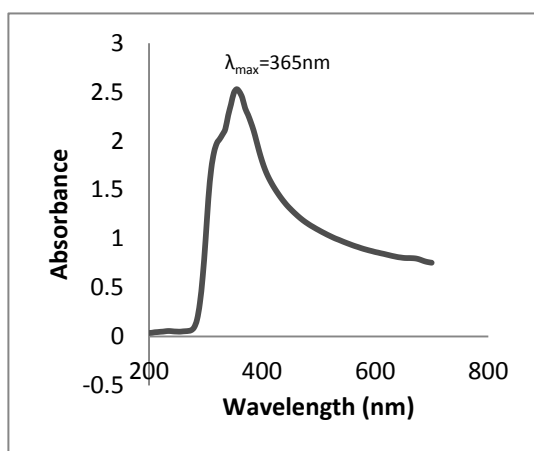


**Figure 1.** UV-visible absorption spectrum of zinc oxide nanoparticles.

The optical band gap was calculated from the absorption spectrum. The energy required for electrons and holes to transition from the valence band to the conduction band is called a band gap. It is also called the energy gap. It changes with the change in particle size. With the decrease in particle size there is an increase in band gap.

The band gap energy ( $E_g$ ) for the ZnO nanoparticles can be calculated by using following equation [39]:

$$E_g = \frac{hc}{\lambda} \text{ eV}$$

where  $E_g$  is band gap energy (eV) of the material,  $h$  refers to Planck's constant ( $6.626 \times 10^{-34}$  Js),  $C$  is the velocity of light ( $3 \times 10^8$  ms<sup>-1</sup>) and  $\lambda$  is the wavelength in nm.

Thus the value of the band gap energy was found to be 3.39 eV which was near the reported value of 3.37 eV [40].

### Effect of Variation of Concentration of Zinc Nitrate

The concentration of the metal precursor used in the synthesis of nanoparticles can notably influence the size of the resulting nanoparticles. In this work, zinc nitrate is taken as a metal precursor for the synthesis of nanoparticles. To study the effect of the concentration of zinc nitrate on the synthesis of zinc oxide nanoparticles, different concentrations of zinc nitrate (1 mM: sample a, 3 mM: sample b, and 5 mM: sample c) were prepared and to each solution, 10 mL of plant extract was added and stirred. After the formation of zinc oxide nanoparticles, the absorption spectra of each sample were taken. From Fig. 2, it was concluded that with an increase in the concentration of zinc nitrate, shifting of the Surface Plasmon Resonance to a longer wavelength (red shift) was observed [41].

The band gap decreased (Table. 1) while increasing the amount of zinc precursor. The decrease in the band gap leads to an increase in the size of the nanoparticles. This showed that the size of nanoparticles increased with the increased amount of zinc precursor. Studies showed that an increase in the concentration of metal precursors may lead to an increase in the size of nanoparticles [42]. Higher precursor concentration provides a greater supply of metal ions available for deposition onto existing nuclei, promoting faster growth. Consequently, higher precursor concentration often leads to larger nanoparticles. The size can be controlled by varying the amount of zinc precursor.

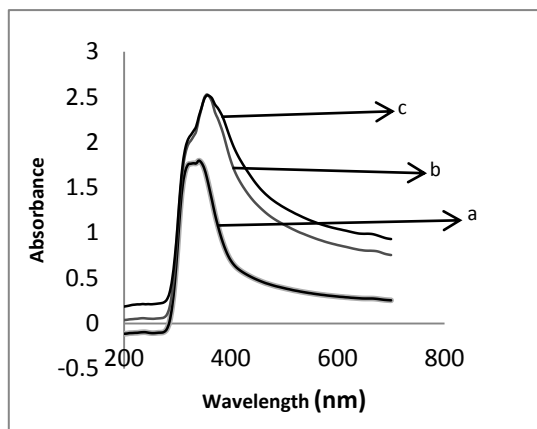


**Figure 2:** UV-Visible spectra of zinc oxide nanoparticles at different concentration of metal precursor: (a) 1 mM, (b) 3 mM and (c) 5 mM.

**Table 1:** Band gap of zinc oxide nanoparticles. (Effect on variation of concentration of zinc nitrate)

Sample	$\lambda_{\max}$ (nm)	Band gap (eV)
A	345	3.59
B	360	3.44
C	365	3.39

### Effect of pH

The size of nanoparticles can be influenced by the acidity or alkalinity (pH) of the surrounding environment. By adjusting the pH of the reaction solution, it is possible to influence the rate of nucleation and growth, which can affect the final size. To study the effect of pH on the formation of zinc oxide nanoparticles, three reaction mixtures were prepared taking 3 mM of zinc nitrate solution and 10 mL of extract. The pH of each reaction mixture was adjusted to 4 (sample a), 8 (sample b), and 9 (sample c). Fig. 3 shows the UV-visible spectrum of ZnO NPs synthesized at various pH conditions. The absorption peak for samples a, b, and c are found at wavelength 355, 365, and 350 nm respectively and their corresponding optical band gap is shown in table 2. With the increase in pH from 4 to 8, the Surface

Plasmon Resonance shifted to a longer wavelength (red shift) and indicated the formation of larger size of zinc oxide nanoparticles, whereas an increase in the pH from 8 to 9 resulted in a shifting of Surface Plasmon Resonance to smaller wavelength (blue shift) due to decrease in the size and polydispersity of nanoparticles [43].

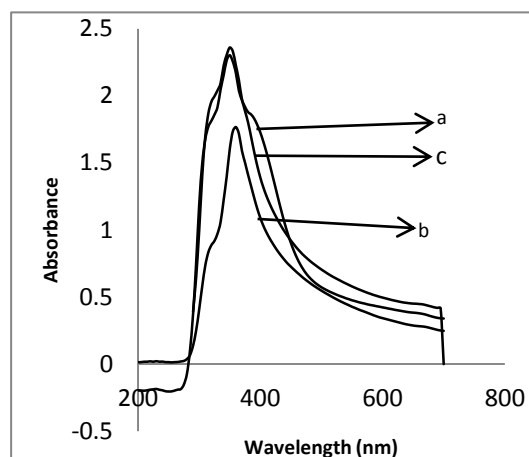


**Figure 3:** UV-Visible spectra of zinc oxide nanoparticles at different pH values; (a) pH 4, (b) pH 8, and (c) pH 9.

**Table 2:** Band Gap of Zinc Oxide Nanoparticles. (Effect of Variation on pH).

Sample	$\lambda_{\max}$ (nm)	Band gap (eV)
A	355	3.49
B	365	3.39
C	350	3.54

### Effect of variation of reduction time

The reaction time can have a significant impact on the size of nanoparticles formed during synthesis. To study the effect of the reduction time on the synthesis of zinc oxide nanoparticles, the reaction mixture with 3 mM of zinc nitrate solution with 20 mL of plant extract was stirred at different time durations. After the formation of zinc oxide nanoparticles, absorption spectra were taken at the duration of 1 hour. Fig. 4

shows the UV-visible spectrum of ZnO NPs synthesized at various reduction times and their corresponding band gap energies are shown in Table 3. It is clear from the absorption spectra that the maximum absorbance wavelength ( $\lambda_{\max}$ ) is red-shifted from 320 to 355 nm by increasing the reaction time. This showed that this red shifting may be due to the increase in size of the nanoparticles by increasing the reaction time (44). After nucleation, the nanoparticles continue to grow by the addition of atoms from the reaction solution. The duration of reaction time can influence the growth rate of the nanoparticles. Longer reaction time may lead to more extensive growth resulting in larger-sized particles.

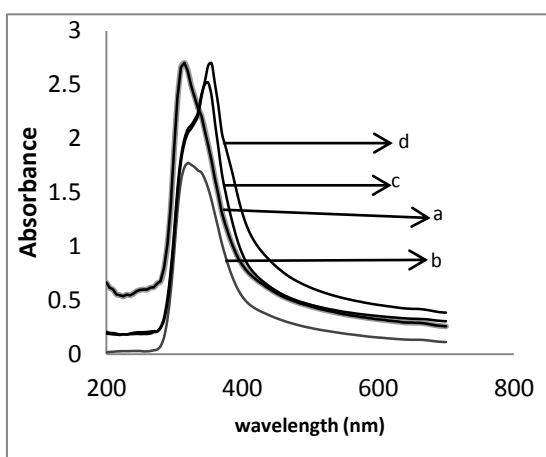


**Figure 4:** UV-Visible spectra of zinc oxide nanoparticles: (a) 1 h, (b) 2 h, (c) 3 h and d) 4 h.

**Table 3:** Band Gap of Zinc Oxide Nanoparticles (Effect of variation of time)

Sample	$\lambda_{\max}$ (nm)	Band gap (eV)
A	320	3.87
B	330	3.75
C	350	3.54
D	355	3.49

## FTIR analysis

The Fourier Transform Infrared Spectra (FTIR) measurement was carried out for the identification of the possible functional groups responsible for the formation of zinc oxide nanoparticles. The extract exhibited peaks (Figure 5) at  $1610\text{ cm}^{-1}$ ,  $2050\text{ cm}^{-1}$ , and  $3250\text{ cm}^{-1}$  due to  $\text{-OH}$  stretching in phenolic compounds, primary amines, and amides (availability of proteins/enzymes). Furthermore, the nanoparticles exhibited an intense band at  $\sim 540\text{ cm}^{-1}$  attributed to the stretching vibration of Zn-O, which confirmed the presence of zinc oxide nanoparticles [45]. The green-synthesized zinc oxide nanoparticles showed several peaks at  $1006\text{ cm}^{-1}$ ,  $1310\text{ cm}^{-1}$ ,  $1620\text{ cm}^{-1}$ , and  $3300\text{ cm}^{-1}$ , due to C-O-C, C-C in aromatic groups, C=O and OH and C-H stretching in phenolic compounds, respectively [46].

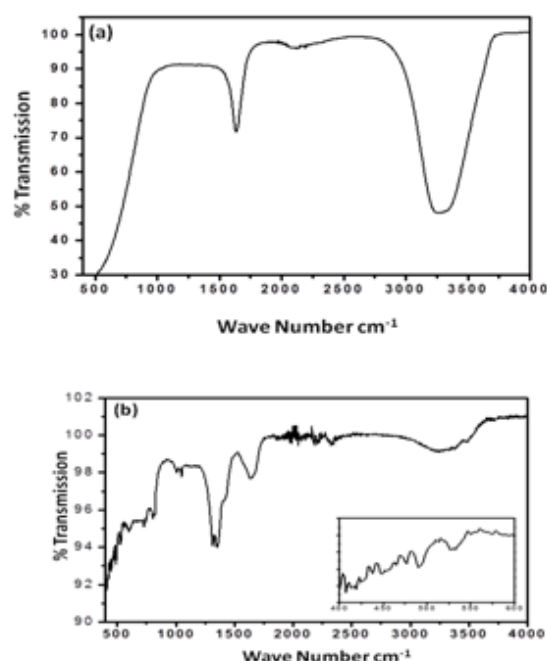


**Figure 5:** FTIR spectra of (a) plant extract and (b) zinc oxide NPs.

## XRD analysis

XRD technique was used to study the size of zinc oxide nanoparticles. Figure 6 depicts XRD analysis of

synthesized ZnO nanoparticles that exhibited peaks appeared at  $2\theta$  values of 31.68, 34.33, 36.15, 47.45, 56.49, 62.76, 66.29, 67.85, 68.99, 72.54 and 76.89 corresponding to Miller indices 100, 001, 101, 102, 110, 103, 200, 112, 201, 004 and 202 respectively matched well with the reference data sheet for zinc oxide nanoparticles in Joint Committee on Powder Diffraction Standards (JCPDS) card no. 36-1451 [47]. XRD pattern showed the crystalline nature of zinc oxide nanoparticles. The crystallite size of the zinc oxide nanoparticles was determined using Scherrer's equation.

$$D = \frac{0.94\lambda}{\beta \cos\theta}$$

where,  $\lambda$  is the wavelength of X-ray (0.154 nm),  $\beta$  = FWHM (full width at half maxima).  $\theta$  = diffraction angle and  $D$  = size. The size of zinc oxide nanoparticles in the range of 7- 14 nm and average size is about 10 nm.

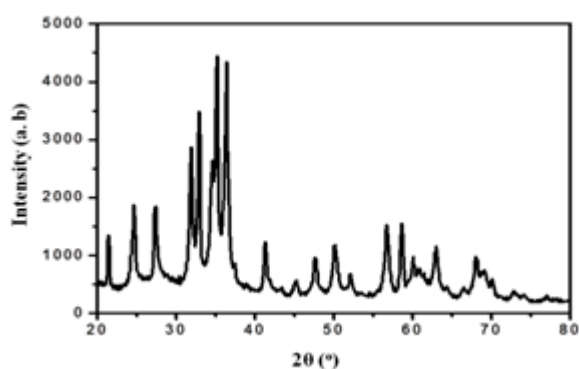


Figure 6: XRD pattern of zinc oxide nanoparticles

### FE-SEM analysis

Field emission scanning electron microscopy (FE-SEM) technique was used to examine the surface morphology of the zinc oxide nanoparticles. FE-SEM images of zinc oxide nanoparticles are shown in Fig.7. The figure shows that the zinc oxide nanoparticles

possess irregular morphology and are agglomerated due to the polarity and electrostatic attraction of nanoparticles.

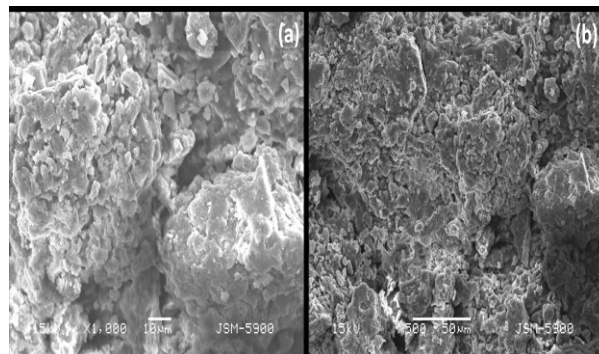


Figure 7: FE-SEM images of zinc oxide nanoparticles

### Antibacterial activity of ZnO nanoparticles

The synthesized ZnO NPs were screened for *in vitro* antibacterial activity against one Gram-positive bacteria (*Staphylococcus aureus*) and three Gram-negative bacteria (*Escherichia coli*, *Salmonella typhimurium* and *Klebsiella pneumoniae*) agar well diffusion method. The results obtained were compared with that of the standard drug neomycin (1  $\mu\text{g}/\text{mL}$ ) as a positive control (PC) and are reported in Table 4 and shown in figure 8 and 9.

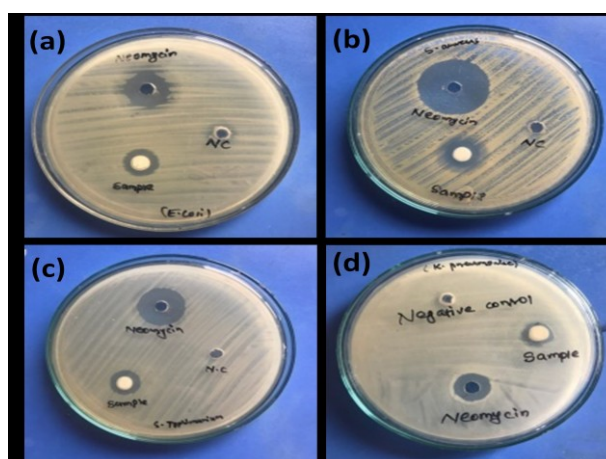
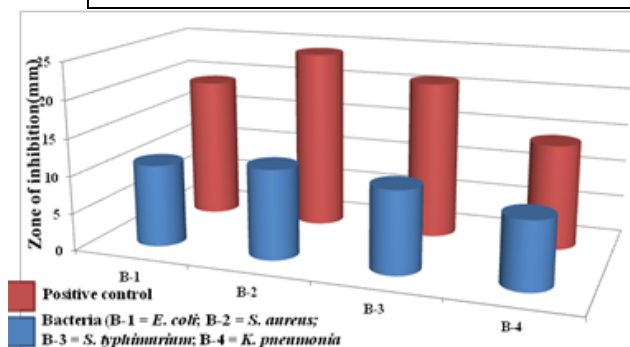


Figure 8: In vitro antibacterial screening of synthesized ZnO NPs showing zone of inhibition

- (a) *Escherichia coli*
- (b) *Staphylococcus aureus*
- (c) *Salmonella typhimurium*
- (d) *Klebsiella pneumoniae*.

Table: 4 Zone of Inhibition ( $\phi = 6\text{mm}$ )

Sample	<i>E. coli</i> (-)	<i>S. aureus</i> (+)	<i>S. typhimurium</i> (-)	<i>K. pneumonia</i> (-)
Zinc oxide NPs	11 mm	12 mm	11 mm	9 mm
Positive Control	19 mm	24 mm	21 mm	14 mm
+ = Gram positive strain and - = Gram negative strain of bacteria				



**Figure 9:** Antibacterial activity of ZnO NPs against different types of bacteria

The observance of an inhibition zone clearly showed the disruption of the membrane, due to zinc oxide nanoparticles with high rates of reactive oxygen species (ROS) generation leading to the death of pathogens [48]. The synthesized nanoparticles were smaller than bacterial pores, and capable of crossing the cell membrane freely.

## Conclusions

Green synthesis of zinc oxide nanoparticles using an aqueous extract of rhizomes of *Acorus calamus* can be reported as an economical, environmentally benign, efficient, and safe method. The aqueous plant extract acted as a reducing agent for the synthesis of ZnO NPs. The formation of ZnO NPs was confirmed by UV-visible spectroscopy. This study showed that the size of nanoparticles can be influenced by the pH, the reduction time, and the concentration of the metal precursor. FTIR showed that the reducing functional

group found in the aqueous extract of rhizomes of the *Acorus calamus* was responsible for the synthesis of ZnO NPs. Furthermore, XRD asserted the formation of crystalline ZnO. The average crystallite size of about 10 nm was calculated using the Scherrer formula for the ZnO NPs. The FE-SEM images show the irregular morphology and agglomerated nanoparticles. Agglomeration of the nanoparticles can be assigned to the polarity and electrostatic force of attraction among the nanoparticles. The as-synthesized nanoparticles showed notable antibacterial activity against *S. aureus* (Gram-positive bacteria) and *E. coli*, *S. typhimurium*, and *K. pneumonia* (Gram-negative bacteria).

## Acknowledgments

The authors acknowledge the facilities rendered by the Department of Chemistry, Amrit College for necessary laboratory facilities, Central Department of Chemistry, Kirtipur for IR spectroscopy, National Academy of Science and Technology (NAST), Lalitpur for XRD, Jeonbuk National University (JNU), Korea for FE-SEM analysis and National Institute of Science and Technology (NIST), Khusibu for anti-bacterial properties.

## References

1. S. Bhatia, Natural Polymer Drug Delivery Systems, Springer International Publishing Switzerland 2016. (DOI: 10.1007/978-3-319-41129-3)
2. A. V. Dijken, D. Meulenkamp, D. Vanmaekelbergh, and A. Meijerink, The luminescence of nanocrystalline zinc oxide nanoparticles: the mechanism of the ultraviolet and visible emission, *Journal of Luminescence*, 2008, **87**, 454-456. (DOI: [10.1016/S0022-2313\(99\)00482-2](https://doi.org/10.1016/S0022-2313(99)00482-2)).
3. S. Ullangula, A. V. Ravindra and S. Ganganaguta, Preparation and characterization of ZnO nanoparticles: application to sensor devices, *Sensors & Transducers*, 2016, **198**(3), 25. (<http://www.sensorsportal.com>).
4. H. E. Brown, *Zinc oxide rediscovered*. Science and Education Publishing, The New Jersey Zinc Company, 1957.
5. Y. S. Kim, W. P. Tai, S. J. Shu, Effect of preheating temperature on structural and optical properties of zinc oxide films by sol-gel process, *Thin Solid Films*, 2005, **491**, 153-160. (DOI: [10.1016/j.tsf.2005.06.013](https://doi.org/10.1016/j.tsf.2005.06.013)).
6. E. Zanni, C. R. Chandraiahgari, G. D. Bellis, and D. Uccelletti, Zinc oxide nano-rods- decorated graphene nano-platelets: a promising antimicrobial agent against the carcinogenic bacterium *Streptococcus mutans*, *Nanomaterials*, 2016,**7**, 179-185. (DOI: [10.3390/nano6100179](https://doi.org/10.3390/nano6100179)).
7. A. Azam, A. S. Ahmed, M. Oves, M. S. Khan, S. S. Habib, and A. Memic, Antimicrobial activity of metal oxide nanoparticles against Gram-positive and Gram-negative bacteria: a comparative study, *International Journal of Nanomedicine*, 2012, **7**, 6003-6009. (DOI: [10.2147/IJN.S35347](https://doi.org/10.2147/IJN.S35347)).
8. J. Sawai, H. Kojima, H. Igarashi, A. Hashimoto, S. Shoji, A. Takehara, and M. Shimizu, *Escherichia coli* damage by ceramic powder slurries, *Journal of Chemical Engineering of Japan*, 1997, **30**(6), 1034-1039. (DOI: [10.1252/jcej.30.1034](https://doi.org/10.1252/jcej.30.1034)).
9. M. Singal, V. Chhabra, P. Kang, and D. O. Shah, Synthesis of ZnO nanoparticles for varistor application using Zn-substituted aerosol or microemulsion, *Materials Research Bulletin*, 1997, **32**(2), 239-247. (DOI: [10.1016/S0025-5408\(96\)00175-4](https://doi.org/10.1016/S0025-5408(96)00175-4)).
10. E. Topoglidis, A. E. Cass, B. O'Regan, and J. R. Durrant, Immobilisation and bioelectrochemistry of proteins on nanoporous TiO<sub>2</sub> and ZnO films, *Journal of Electroanalytical Chemistry*, 2001, **517**(1-2), 20-27. (DOI: [10.1016/S0022-0728\(01\)00673-8](https://doi.org/10.1016/S0022-0728(01)00673-8)).
11. P. V. Kamat, Manipulation of charge transfers across semiconductor interface. A criterion that cannot be ignored in photocatalyst design, *The Journal of Physical Chemistry Letters*, 2012, **3**(5), 663-672. (DOI: [10.1021/jz201629p](https://doi.org/10.1021/jz201629p)).
12. X. L. Cheng, H. Zhao, L. H. Huo, S. Gao, and J. G. Zhao, Zinc oxide particulate thin films: preparation, characterization, and gas-sensing properties, *Journal of Chemistry*, 2004, **102**, 248-252. (DOI: [10.1016/j.snb.2004.04.080](https://doi.org/10.1016/j.snb.2004.04.080)).
13. C. Dagdeviran, S. W. Hwang, Y. Su, S. Kim and J. A. Rogers, Transient, biocompatible electronics and energy harvesters based on zinc oxide, *Journal of Nanoparticles*, 2013, **9**, 3398-3404. (DOI: [10.1002/sml.201300146](https://doi.org/10.1002/sml.201300146)).

14. H. Mirzaei and M. Darroudi, Zinc oxide nanoparticles: Biological synthesis and biomedical applications, *Ceramics International*, 2017, **43**(1), 907-914. (DOI: 10.1016/j.ceramint.2016.10.051)
15. K. Matsubara, P. Fon, K. Iwata, A. Yamada, K. Sakurai, H. Tampo, S. Niki, Zinc oxide transparent films deposited by pulsed laser deposition for solar cell applications, *Thin Solid Films*, 2003, **431**, 369-372. (DOI: 10.1016/S0040-6090(03)00243-8).
16. K. T. Dhermendre, and J. Behari, Application of nanoparticles in waste water treatment, *World Applied Science Journal*, 2008, **3**(3), 417-433. (ISSN 1818-4952, IDOSI Publications).
17. S. H. Cha, J. Hong, M. McGuffie, B. Yeom, J. S. VanEpps, and N. A. Kotov, Shape-dependent biomimetic inhibition of enzyme by nanoparticles and their antibacterial activity, *American Chemical Society Nano*, 2015, **9**(9), 9097-9105. (DOI: 10.1021/acs.nano.5b03247)
18. G. Baskar, J. Chandhuru, K. S. Fahad, A. S. Praveen, M. Chamundeeswari and T. Muthukumar, Anticancer activity of fungal *L-asparaginase* conjugated with zinc oxide nanoparticles, *Journal of Materials Science: Materials in Medicine*, 2015, **26**(1), 43-50. (DOI: 10.1007/s10856-015-5380-z)
19. K. Parveen, V. Banse, and L. Ledwani, Green synthesis of nanoparticles: Their advantages and disadvantages, *AIP Conference Proceedings*, 2015, **1724**(1), 020048. (DOI: 10.1063/1.4945168).
20. V. Parashar, R. Parashar, B. Sharma, and A. C. Pandey, Parthenium leaf extract mediated synthesis of silver nanoparticles: a novel approach towards weed utilization, *Digest Journal of Nanomaterials & Biostructures (DJNB)*, 2009, **4**(1), 45-50. (<https://www.researchgate.net/publication/216540414>)
21. N. Saifuddin, C. W. Wong, and A. Yasumira, Rapid biosynthesis of silver nanoparticles using culture supernatant of bacteria with microwave irradiation, *Journal of Chemistry*, 2009, **6**(1), 61-70. (DOI: 10.1155/2009/734264).
22. K. Bhainsa, and S. Sauza, Extracellular biosynthesis of silver nanoparticles using seed extract of *Jatropha curcas*, *Colloids Surface Chemistry*, 2006, **47**, 160-164. (DOI: 10.1016/j.colsurfb.2005.11.026).
23. I. Willner, B. Basnar, and B. Willner, Nanoparticle-enzyme hybrid systems for nanobiotechnology, *The Febs Journal*, 2017, **274**, 302-309. (DOI: 10.1111/j.1742-4658.2006.05602.x.).
24. S. Joghee, G. Pradheesh, V. Alexramani, M. Sundrarajan, and H. I. Hong, Green synthesis and characterization of zinc oxide nanoparticles using insulin plant (*Costus pictus* D. Don) and investigation of its antimicrobial as well as anticancer activities, *Advances in Natural Sciences: Nanoscience and Nanotechnology*, 2018, **9**(1), 015008. (DOI: 10.1088/2043-6254/aaa6f1)
25. T. S. Anvekar, V. R. Chari, and H. Kadam, Green synthesis of ZnO nanoparticles, its characterization and application, *Material Science Research India*, 2017, **14**(2), 153-157. (DOI: 10.13005/msri/140211)
26. Y. Zheng, L. Fu, F. Han, A. Wang, W. Cai, J. Yu, and F. Peng, Green biosynthesis and characterization of zinc oxide nanoparticles using *Corymbia citriodora* leaf extract and their photocatalytic activity, *Green Chemistry Letters and Reviews*, 2015, **8**(2), 59-63. (DOI: 10.1080/17518253.2015.1075069)
27. K. Lingaraju, H. R. Naika, K. Manjunath, R. B. Basavaraj, H. Nagabhushana, G. Nagaraju, D. Suresh, Biogenic synthesis of zinc oxide nanoparticles using *Ruta graveolens* (L.) and their antibacterial and antioxidant activities, *Applied Nanoscience*, 2016, **6**(5), 703-710. (DOI: 10.1007/s13204-015-0487-6)

28. D. Mahendiran, G. Subash, D. A. Selvan, D. Rehana, R. S. Kumar, and A. K. Rahiman, Biosynthesis of zinc oxide nanoparticles using plant extracts of aloe vera and *Hibiscus sabdariffa*: phytochemical, antibacterial, antioxidant and anti-proliferative studies, *BioNanoScience*, 2017, **7**(3), 530-545. (DOI: 10.1007/s12668-017-0418-y).
29. M. Aminuzzaman, L. P. Ying, W. S. Goh, and A. Watanabe, Green synthesis of zinc oxide nanoparticles using aqueous extract of *Garcinia mangostana* fruit pericarp and their photocatalytic activity, *Bulletin of Materials Science*, 2018, **41**(2), 41-50. (DOI: 10.1007/s12034-018-1568-4).
30. B. Baskaran, S. K. NC, S. Chindambaram and K. Ramachandran, Synthesis and characterization of zinc oxide nanoparticles using marine *Streptomyces* sp. with its investigations on anticancer and antibacterial activity, *Research on Chemical Intermediates*, 2017, **43**(4), 2367-2376. (DOI: 10.1007/s11164-016-2766-6).
31. R. Ishwarya, B. Vaseeharan, S. Kalyani, B. Banumathi, M. Govindarajan, N. S. Alharbi, G. Benelli, Facile green synthesis of zinc oxide nanoparticles using *Ulva lactuca* seaweed extract and evaluation of their photocatalytic, antibiofilm and insecticidal activity, *Journal of Photochemistry and Photobiology B: Biology*, 2018, **178**, 249-258. (DOI: 10.1016/j.jphotobiol.2017.11.006).
32. D. K. Slman, R. D. A. Jalill and A. N. Abd, Biosynthesis of zinc oxide nanoparticles by hot aqueous extract of *Allivum sativum* plants, *Journal of Pharmaceutical Sciences and Research*, 2018, **10**(6), 1590-1596. (<https://www.researchgate.net/publication/326395100>)
33. A. Alaghemand, S. Khagani, M. R. Bihamta, M. Gomarian and M. Ghorbanpour, Green synthesis of zinc oxide nanoparticles using *Nigella sativa* L. extract: The effect on the height and number of branches, *Journal of nanostructures*, 2018, **8**(1), 82-88. (DOI: 10.22052/JNS.2018.01.010)
34. R. Balakumbahan, K. Rajamani, K. Kumanan, *Acorus calamus*: An overview, *Journal of Medicinal Plants Research*, 2010, **4**(25), 2740-2745. (DOI: doi.org/10.5897/JMPR.9000038).
35. R. Ramy, F. Sayed and M. Ghada, Chemical compositions, antiviral and antioxidant activities of several essential oils, *Journal of Applied Science Research*, 2010, **6**, 50-62. (<https://www.researchgate.net/publication/234004581>)
36. K. Manjunath, K. Lingaraju, D. Kumar, H. Nagabhushan, D. Samrat, V. Reddy and G. Nagaraju, Electrochemical sensing of dopamine and antibacterial properties of ZnO nanoparticles synthesized from solution combustion method, *International Journal of Nanoscience*, 2015, **14**(03), 1550005. (DOI: 10.1142/S0219581X15500052).
37. K. Elumalai, S. Velmurugan, S. Ravi, V. Kathiravan, S. A. Kumar, Bio-fabrication of zinc oxide nanoparticles using leaf extract of curry leaf (*Murraya koenigii*) and its antimicrobial activities, *Materials Science in Semiconductor Processing*, 2015, **34**, 365-372. (DOI: 10.1016/j.mssp.2015.01.048).
38. A. K. Zak, W. H. Majid, M. R. Mahmoudian and M. Darroudi, Starch stabilized synthesis of ZnO nano powders at low temperature and optical properties study, *Advanced Powder Technology*, 2013, **24**, 496-502. (DOI: 10.1016/j.appt.2012.11.008).
39. E. Wagner, Investigating band gap energies, materials, and design of light-emitting diodes, *Journal of Chemical Education*, 2016, **93**(7), 1289-1298. (DOI:10.1021/acs.jchemed.6b00165).

40. A. Vasudevan, S. Jung, and T. Ji, Synthesis and characterization of hydrolysis grown zinc oxide nanorods, *International Scholarly Research Network*, 2011, **1**, 1-7. (DOI: 10.5402/2011/983181).
41. D. Dorranaiana, and A. F. Eskandari, Effect of laser fluence on the characteristics of zinc oxide nanoparticles produced by laser ablation in acetone, *Molecular Crystals and Liquid Crystals*, 2015, **607**(1), 1-12. (DOI: 10.1080/15421406.2014.927414).
42. H. S. Dehsari, A. H. Ribeiro, B. Ersoz, W. Tremel, G. Jakola and K. Asadi, Effect of precursor concentration on size evolution of iron oxide nanoparticles, *CrystEngComm*, 2017, **19**, 6694–6702. (DOI: 10.1039/C7CE01406F).
43. L. Marciniak, M. Nowak, A. Trojanowska, B. Tylkowski, and R. Jastrzab, The effect of pH on the size of silver nanoparticles obtained in the reduction reaction with citric and malic acids, *Materials*, 2020, **13**, 5444-5455. (DOI: 10.3390/ma13235444).
44. S. Shrestha and S. Adhikari, Size dependent optical properties of silver nanoparticles synthesized from fruit extract of *Malus pumila*, *Journal of Nepal Chemical Society*, 2017, **37**, 43-48. (DOI: 10.3126/jncs.v37i0.32111).
45. S. K. Mandal, A. K. Das, T. K. Nath, and D. Karmakar, Temperature dependence of solubility limits of transition metals (Co, Mn, Fe, and Ni) in ZnO nanoparticles, *Applied Physics Letters*, 2006, **89**(14), 144105. (DOI:10.1063/1.2360176).
46. Kwak, D. H., Lee, Y. W., Han, S. B., Lee, J. Y., Zhoh, C. K., & Park, K. W. (2015). Electrocatalytic oxidation reactions of platinum hexapod nanoparticles, *Electrochimica Acta*, 2015, **176**, 790-796. (DOI: <https://doi.org/10.1016/j.electacta.2015.07.075>).
47. S. Umavathi, S. Mahboob, M. Govindarajan, K. A. Al-Ghanim, Z. Ahmed, P. Virik, N. Al-Mulhm, M. Subash, K. Gopinath, and C. Kavitha, Green synthesis of ZnO nanoparticles for antimicrobial and vegetative, *Saudi Journal of Biological Sciences*, 2021, **28**, 1808-1815. (DOI: 10.1016/j.sjbs.2020.12.025).
48. T. Jin, D. Sun, J. Y. Su, H. Zhang and H. J. Sue, Antimicrobial efficacy of zinc oxide quantum dots against *Listeria monocytogenes*, *Salmonella enteritidis*, and *Escherichia coli*, *Journal of Food Science*, 2009, **74**(1), 46-52. (DOI: 10.1111/j.1750-3841.2008.01013.x).